Molecular Therapy
Methods & Clinical Development
Original Article

Impact of an autophagy-inducing peptide on immunogenicity and protection efficacy of an adenovirus-vectored SARS-CoV-2 vaccine

Ekramy E. Sayedahmed,[1,10,11,13] Marcelo Valdemir Araújo,[2,3,13] Taiana Tainá Silva-Pereira,[2,13] Shubhada K. Chothe,[8,13] Ahmed Elkashif,[1,10,11] Marwa Alhashimi,[1,10,11] Wen-Chien Wang,[1,10,11] Andrea P. Santos,[1,10,11] Meera Surendran Nair,[6,9] Abhinay Gontu,[8] Ruth Nissly,[9] Antônio Francisco de Souza Filho,[2] Mariana Silva Tavares,[2] Marina Caçador Ayupe,[4] Caio Loureiro Salgado,[4] Érika Donizetti de Oliveira Candido,[2] Danielle Bruna Leal Oliveira,[2] Edison Luiz Durigon,[2] Marcos Bryan Heinemann,[5] Denise Morais da Fonseca,[4] Chinnaswamy Jagannath,[7,12] Ana Marcia Sá Guimarães,[2] Suresh V. Kuchipudi,[9] and Suresh K. Mittal[1,10,11]

[1]Department of Comparative Pathobiology, College of Veterinary Medicine, Purdue University, West Lafayette, IN, USA; [2]Department of Microbiology, Institute of Biomedical Sciences, University of São Paulo, São Paulo, Brazil; [3]Butantan Institute, São Paulo, Brazil; [4]Department of Immunology, Institute of Biomedical Sciences, University of São Paulo, São Paulo, Brazil; [5]Department of Preventive Veterinary Medicine and Animal Health, College of Veterinary Medicine, University of São Paulo, São Paulo, Brazil; [6]Department of Veterinary and Biomedical Sciences, Huck Institutes of the Life Sciences, Pennsylvania State University, University Park, PA, USA; [7]Department of Pathology and Genomic Medicine, Center for Infectious Diseases and Translational Medicine, Houston Methodist Research Institute, Houston, TX, USA; [8]Department of Veterinary and Biomedical Sciences, Pennsylvania State University, University Park, PA, USA; [9]Animal Diagnostic Laboratory, Department of Veterinary and Biomedical Sciences, Pennsylvania State University, University Park, PA, USA; [10]Purdue Institute of Inflammation, Immunology, and Infectious Disease, Purdue University, West Lafayette, IN, USA; [11]Institute for Cancer Research, Purdue University, West Lafayette, IN, USA; [12]Weill Cornell Medical College, New York, NY, USA

Because of continual generation of new variants of severe acute respiratory syndrome coronavirus 2 (SARS-CoV-2), it is critical to design the next generation of vaccines to combat the threat posed by SARS-CoV-2 variants. We developed human adenovirus (HAd) vector-based vaccines (HAd-Spike/C5 and HAd-Spike) that express the whole Spike (S) protein of SARS-CoV-2 with or without autophagy-inducing peptide C5 (AIP-C5), respectively. Mice or golden Syrian hamsters immunized intranasally (i.n.) with HAd-Spike/C5 induced similar levels of S-specific humoral immune responses and significantly higher levels of S-specific cell-mediated immune (CMI) responses compared with HAd-Spike vaccinated groups. These results indicated that inclusion of AIP-C5 induced enhanced S-specific CMI responses and similar levels of virus-neutralizing titers against SARS-CoV-2 variants. To investigate the protection efficacy, golden Syrian hamsters immunized i.n. either with HAd-Spike/C5 or HAd-Spike were challenged with SARS-CoV-2. The lungs and nasal turbinates were collected 3, 5, 7, and 14 days post challenge. Significant reductions in morbidity, virus titers, and lung histopathological scores were observed in immunized groups compared with the mock- or empty vector-inoculated groups. Overall, slightly better protection was seen in the HAd-Spike/C5 group compared with the HAd-Spike group.

INTRODUCTION

A novel coronavirus (CoV), severe acute respiratory syndrome CoV 2 (SARS-CoV-2), emerged in Wuhan, China, causing the CoV disease 2019 (COVID-19) pandemic.[1] So far, the ongoing pandemic has infected more than 690 million people, with over 6.8 million deaths worldwide.[2] Several COVID-19 vaccines have been tested in preclinical and clinical settings.[3,4] Notably, COVID-19 vaccines based on mRNA,[5] DNA,[6] inactivated virus,[7] subunits,[8] and adenovirus (Ad) vectors[9] are currently being used in humans globally. All of these vaccines are based on the Spike (S) glycoprotein, an excellent target for virus-neutralizing antibodies. The S glycoprotein (~180 kDa) of SARS-CoV-2 is cleaved by a furin protease into N-terminal S1 and C-terminal S2 subunits.[10–12] The S1 subunit contains the receptor-binding domain (RBD), a primary target for neutralizing antibodies, whereas the S2 subunit induces membrane fusion. The RBD on the S1 subunit interacts with the angiotensin-converting enzyme 2 (ACE2) receptor on the host cell membrane for virus internalization.[13–17] The identification of neutralizing antibody[18]

Received 24 March 2023; accepted 23 June 2023;
https://doi.org/10.1016/j.omtm.2023.06.009.

[13]These authors contributed equally

Correspondence: Ana Marcia Sá Guimarães, Department of Microbiology, Institute of Biomedical Sciences, University of São Paulo, São Paulo, Brazil.
E-mail: anamarcia@usp.br
Correspondence: Suresh V. Kuchipudi, Animal Diagnostic Laboratory, Department of Veterinary and Biomedical Sciences, Pennsylvania State University, University Park, PA, USA.
E-mail: svk11@psu.edu
Correspondence: Suresh K. Mittal, Department of Comparative Pathobiology, College of Veterinary Medicine, Purdue University, 625 Harrison St, West Lafayette, IN 47907-2027, USA.
E-mail: mittal@purdue.edu

and CD4 and CD8 T cell responses in recovered patients[18] suggests the importance of the S1 subunit as the primary target for developing an effective vaccine.

Various countries are undergoing a fourth or fifth wave of the CoV pandemic because of the emergence of SARS-CoV-2 variants. These variants are classified as Alpha, Beta, Gamma, Delta, Epsilon, Eta, Iota, Kappa, Mu, and Zeta and variants of concern, like Omicron and its descendant lineages.[19,20] The Omicron variants are of significant concern globally because of their transmissibility and less effective treatment with the current monoclonal antibody therapies.[21] Currently used vaccines also elicit markedly lower neutralizing antibody titers against Omicron variants than other variants.[22]

Over 100 COVID-19 vaccines have been developed,[4] and several are in clinical trials in different countries. The extensive use of mRNA-based or Ad vector-based COVID-19 vaccines suggests that the next generation of CoV vaccines will be vital for successfully targeting the virus variants.[23]

We identified the 22-amino-acid residue autophagy-inducing peptide C5 (AIP-C5) of *Mycobacterium tuberculosis* (Mtb) that boosts T cell immune responses to an Mtb 85B epitope[24] or nucleoprotein (NP) of influenza virus.[25] In this study, we explored the usefulness of AIP-C5 with the S protein of SARS-CoV-2, augmenting S-specific cell-mediated immune (CMI) responses and providing better protective efficacy against SARS-CoV-2. Mice or golden Syrian hamsters immunized intranasally (i.n.) with the human adenovirus (HAd) vector expressing SARS-CoV-2 S with AIP-C5 (HAd-Spike/C5) resulted in similar levels of humoral but significantly higher levels of CMI responses compared with the animal groups vaccinated i.n. with the HAd vector expressing only the S protein (HAd-Spike). Golden Syrian hamsters immunized i.n. once with HAd-Spike/C5 had superior protection following challenge with SARS-CoV-2 compared with the group vaccinated with HAd-Spike, as evidenced by reduced viral titers in the nasal turbinate and lungs and lower histopathology scores. The results suggest the importance of AIP-C5 in inducing improved CMI responses against SARS-CoV-2 S.

RESULTS

Development of Ad vectors expressing Spike or Spike/C5

The HAd-Spike and HAd-Spike/C5 vectors carrying the S gene of the Wuhan strain of SARS-CoV-2 (accession number MN908947) without or with AIP-C5 were developed (Figure 1A). The vectors' initial characterization was done by restriction analysis of the genome and sequencing the region containing the gene cassette. Subsequently, the expression of S or S/C5 in vector-infected cell extracts was examined by immunoblot assay using an S-specific mouse monoclonal antibody (GeneTex, GTX632604). Similarly prepared mock- or HAd-ΔE1E3 (empty vector)-infected cell extracts were used as negative controls. Bands of ~80 kDa are for S2 or S2/C5 subunits, and ~150-kDa bands are for S or S/C5 proteins, confirming expresssion of S or S/C5 in HAd-Spike-infected or HAd-Spike/C5-infected cell extract (Figure 1B). To avoid potential interference with the signal peptide of the S protein, AIP-C5 was added at the C-terminal end.

Development of humoral and CMI responses in mice immunized i.n. with HAd-Spike or HAd-Spike/C5

The outlines of one-dose (1D) or two-dose (2D) study designs are presented (Figure 1C). The BALB/c mouse groups were vaccinated i.n. once or twice (with a 4-week interval) with 1× phosphate-buffered saline (PBS) or 1×10^8 plaque-forming units (PFUs) of HAd-ΔE1E3 (human Ad type 5 E1- and E3-deleted empty vector), HAd-Spike, or HAd-Spike/C5. High levels of S-specific immunoglobulin G (IgG), IgG1, IgG2a, and IgA ELISA titers were detected in sera of mouse groups vaccinated once with HAd-Spike or HAd-Spike/C5 (Figures 2A–2D). There were no appreciable increases in S-specific IgG, IgG1, IgG2a, and IgA ELISA titers in sera of mouse groups vaccinated twice, either with HAd-Spike or HAd-Spike/C5. The induction of S-specific antibody responses at the mucosal surface was also monitored. Again, high levels of S-specific IgG, IgG1, IgG2a, and IgA ELISA titers were detected in lung washes of mouse groups vaccinated once with HAd-Spike or HAd-Spike/C5 (Figures 2E–2H). Similarly, there were no appreciable increases in S-specific IgG, IgG1, IgG2a, and IgA ELISA titers in lung washes of mouse groups vaccinated twice with HAd-Spike or HAd-Spike/C5. The control groups inoculated with PBS or HAd-ΔE1E3 did not elicit antigen-specific antibody levels above the background (Figures 2A–2H). The failure to observe a significant boost in antigen-specific antibodies in 2D groups could be due to maximization of the induction of S-specific humoral immune responses following the first dose of the vaccine. The comparative S-specific IgG2a and IgG1 titers suggest development of Th1- and Th2-type immune responses. The high levels of IgA antibodies, especially in the lung wash, strongly indicated development of a mucosa-specific immune response in the HAd-Spike and HAd-Spike/C5 groups.

Previously, we have elucidated that inclusion of AIP-C5 with a bacterial antigen significantly enhances antigen-specific T cell responses.[24] To explore whether animals vaccinated with HAd-Spike/C5 have higher S-specific CMI responses compared with the group immunized with HAd-Spike, the splenocytes, mediastinal lymph node (MLN) cells, and lung mononuclear (MN) cells were analyzed for antigen-specific T cell response by ELISpot. In the 1D and 2D groups, there were significantly increased numbers of S-specific interferon γ (IFN-γ)-secreting T cells in splenocytes (Figure 2I), MLN cells (Figure 2J), and lung MN cells (Figure 2K) in the HAd-Spike/C5 groups compared with the HAd-Spike groups. The higher levels of S-specific T cell responses were attributed to AIP-C5. In the 2D vaccine groups, there were higher numbers of S-specific IFN-γ-secreting T cells in splenocytes (Figure 2I), MLN cells (Figure 2J), and lung MN cells (Figure 2K) compared with the 1D vaccine groups. The control groups inoculated with PBS or HAd-ΔE1E3 did not elicit antigen-specific T cell responses above background levels (Figures 2I–2K).

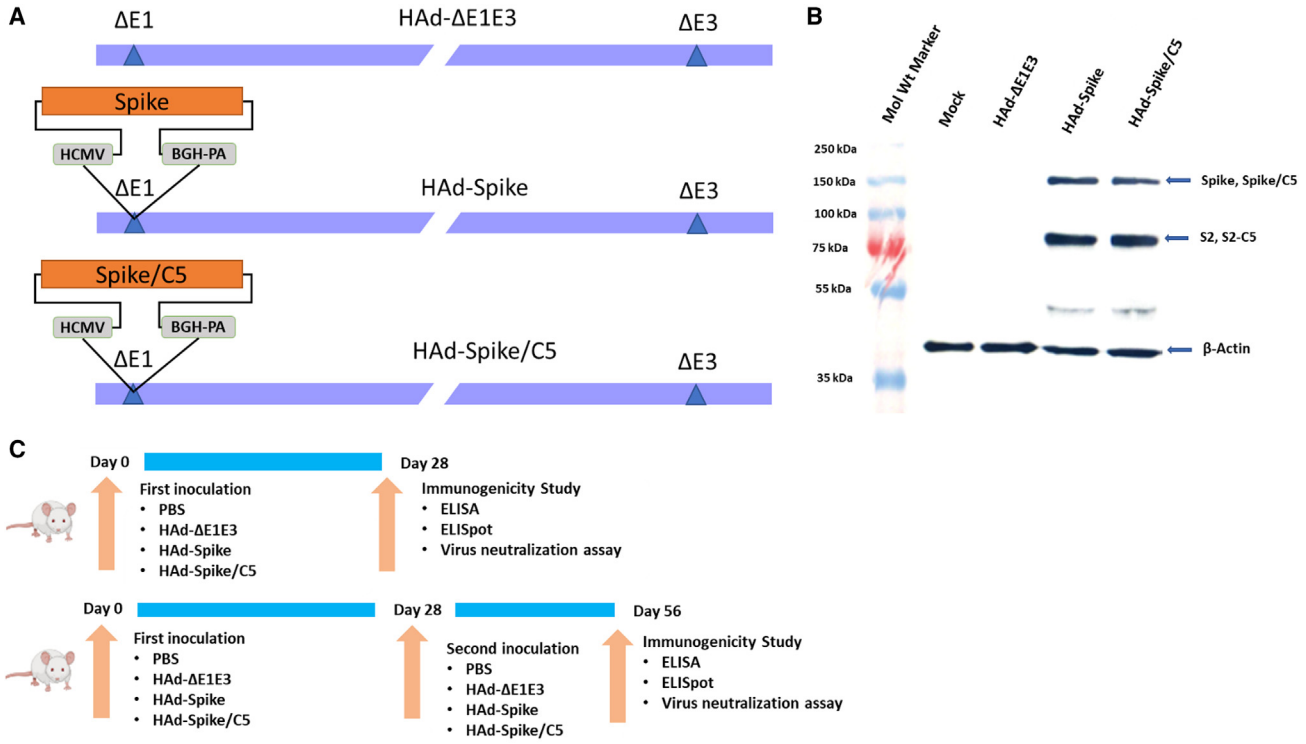

Figure 1. Generation of adenovirus vectored vaccines and mouse study design

(A) Diagrammatic representation of the genomic structures of HAd-ΔE1E3, HAd-Spike, and HAd-Spike/C5. The gene cassettes (SARS-CoV-2 Spike or Spike/C5) were under control of the cytomegalovirus (CMV) promoter and the bovine growth hormone (BGH) polyadenylation signal. The illustrations are not to scale. ΔE1, deletion of the E1 region; ΔE3, deletion of the E3 region; C5, C5-AIP. (B) Immunoblot of 293 cells infected with HAd-Spike or HAd-Spike/C5 to demonstrate expression of Spike or Spike/C5. Mock- or HAd-ΔE1E3-infected cell extracts were used as negative controls. The molecular weight marker is shown on the left. The immunoblotting for β-actin was performed to confirm an equal amount of protein loading in each well. (C) Outlines of 1D (top panel) and 2D (bottom panel) immunogenicity studies in mice.

Induction of virus-neutralizing antibodies against SARS-CoV-2 variants in mice immunized i.n. with HAd-Spike or HAd-Spike/C5

Levels of SARS-CoV-2-neutralizing antibodies provide evidence of expected protection efficacy.[26,27] To determine virus neutralization antibodies against hCoV-19/USA-WA1/2020 (Wuhan), hCoV-19/England/204820464/2020 (B.1.1.7; Alpha), hCoV-19/South Africa/KRISP-K005325/2020 (lineage B.1.351; Beta), hCoV-19/Brazil P.1 (B.1.1.28; Gamma), hCoV-19/USA/PHC658/2021 (lineage B.1.617.2; Delta), or hCoV-19/USA/MD-HP20874/2021 (lineage B.1.1.529; Omicron), serum samples from immunized mice were used for a virus neutralization assay. All SARS-CoV-2 variants were obtained from BEI Resources (Manassas, VA, USA). Because the vaccine vectors contained the S gene of the Wuhan strain, mouse groups immunized with HAd-Spike or HAd-Spike/C5 had mean virus neutralization titers of $\sim 10^4$ against the homologous strain (Figure 3A). Significantly high levels of virus neutralization titers against Alpha (Figure 3B), Beta (Figure 3C), Gamma (Figure 3D), and Delta (Figure 3E) were observed in the immunized groups; however, these titers were approximately one log down compared with the virus neutralization titers with the Wuhan strain. Virus neutralization titers against the Omicron variant were about two logs down compared with the Wuhan strain (Figure 3F). There were no significant differences in virus neutralization titers in animal groups immunized once (1D) or twice (2D). No significant differences in virus neutralization titers were observed in the groups vaccinated with HAd-Spike or HAd-Spike/C5.

Development of humoral and CMI responses in golden Syrian hamsters immunized i.n. with HAd-Spike or HAd-Spike/C5

Golden Syrian hamsters are an excellent small animal model for assessing SARS-CoV-2 pathogenesis and evaluating vaccine efficacy.[28,29] Because our mouse studies did not demonstrate significantly enhanced levels of humoral immune responses in the 2D group compared with the 1D group, we chose to evaluate the immunogenicity of HAd-Spike or HAd-Spike/C5 in golden Syrian hamsters only as a 1D regimen. The outlines of immunogenicity and challenge studies are presented in Figure 4A. The serum samples from hamsters immunized with HAd-Spike or HAd-Spike/C5 developed similar S-specific IgG and IgG2/IgG3 titers (Figures 4B and 4C), suggesting that inclusion of AIP-C5 did not have an impact on humoral immunity. Similar S-specific IgG and IgG2/IgG3 ELISA titers were detected in lung washes of groups vaccinated with HAd-Spike or HAd-Spike/C5 (Figures 4D and 4E). The control group inoculated with HAd-ΔE1E3 did not elicit antigen-specific antibody levels above the background (Figures 4B–4E). IgG2 and IgG3 cross react in the hamster

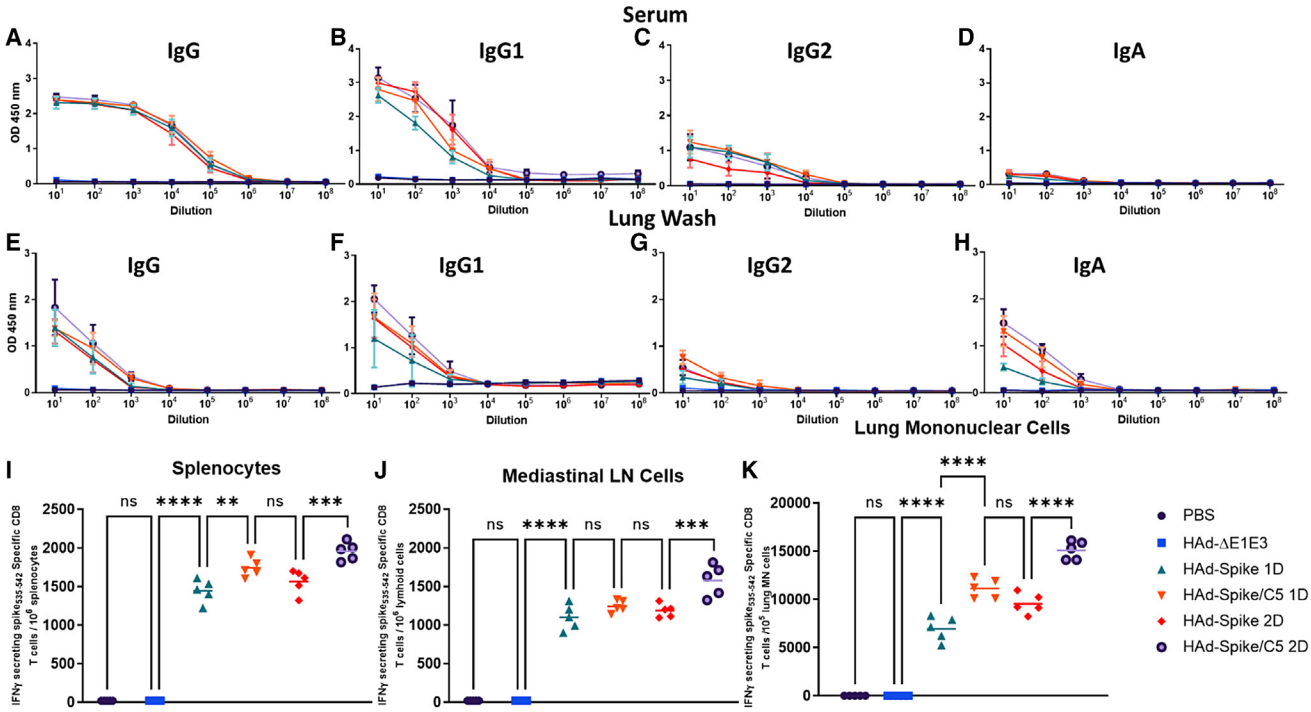

Figure 2. Immunogenicity of HAd-Spike and HAd-Spike/C5 in mice

Six- to eight-week-old BALB/c mice (5 animals/group) were mock inoculated (PBS) or inoculated intranasally (i.n.) once (1D) or twice (2D) with 10^8 PFUs/animal of HAd-ΔE1E3, HAd-Spike, or HAd-Spike/C5. (A–D) Four weeks post immunization, blood samples were used to study the development of Spike-specific IgG (A), IgG1 (B), IgG2a (C), and IgA (D) antibody responses by ELISA. (E–H) Similarly, lung washes were used for monitoring the development of Spike-specific IgG (E), IgG1 (F), IgG2a (G), and IgA (H) antibody responses by ELISA. ELISA data are shown as the mean ± standard deviation (SD) of the optical density (OD) readings with log10 diluted samples. (I–K) The development of a Spike-specific T cell response after vaccination was investigated in splenocytes (I), mediastinal lymph node (MLN) cells (J), and lung MN cells (K) by counting Spike-specific IFN-γ-secreting CD8 T cells by ELISpot. ns, non-significant, $p > 0.05$; *$p < 0.05$; **$p < 0.01$; ***$p < 0.001$; ****$p < 0.0001$. 1D, one dose; 2D, two doses.

because they share the H band. They are good indicators of the quality of immune responses following immunization.[30]

To investigate whether hamsters vaccinated with HAd-Spike/C5 will have higher levels of S-specific CMI responses compared with the group immunized with HAd-Spike, splenocytes, peripheral blood MN cells (PBMCs), and lung MN cells were analyzed for antigen-specific T cell responses by ELISpot. There were significantly high numbers of S-specific IFN-γ-secreting T cells in splenocytes (Figure 4F), PBMCs (Figure 4G), and lung MN cells (Figure 4H) in the HAd-Spike/C5 group compared with the HAd-Spike group, indicating a role of AIP-C5 in enhancing T cell responses. The control groups inoculated similarly with HAd-ΔE1E3 did not elicit antigen-specific T cell responses above the background (Figures 4F–4H).

The serum samples from immunized hamsters were also used for determining virus neutralization antibodies against hCoV-19/USA-WA1/2020 (Wuhan). The mean virus-neutralizing titers in the group vaccinated with HAd-Spike or HAd-Spike/C5 were 506.0 and 506.7, respectively (Figure 5A), suggesting that AIP-C5 did not enhance development of a virus-neutralizing antibody response.

Protection efficacy of golden Syrian hamsters immunized with HAd-Spike or HAd-Spike/C5 following challenge with SARS-CoV-2

Golden Syrian hamsters immunized with HAd-Spike or HAd-Spike/C5 were challenged with SARS-CoV-2 (B.1.1.28) 35 days post vaccination to evaluate protective efficacy. Our choice for the challenge virus was based on the fact that B.1.1.28 was the predominant strain in Brazil at the time of this study, and we were looking for a different variant than Wuhan. Morbidity (weight loss) and virus titers in the nasal turbinate and lungs were used to measure protection efficacy. Minimum morbidity was observed in the groups immunized with HAd-Spike (3.8% average weight loss on day 4 post challenge) or HAd-Spike/C5 (1.3% average weight loss on day 2 post challenge) compared with the morbidity of the non-infected PBS group (Figure 5B). In contrast, infected control groups inoculated with PBS or HAd-ΔE1E3 showed significantly higher morbidity (nearly 7%–9% average weight loss on days 6 and 7 post challenge) than the non-infected and the vaccinated groups between day 4 and day 10 after infection (Figure 5B). The animal groups immunized with HAd-Spike or HAd-Spike/C5 had significantly lower virus titers in the lungs (Figures 5C and 5D) and nasal turbinate (Figures 5E and 5F) compared with the PBS or HAd-ΔE1E3 group. There were slightly

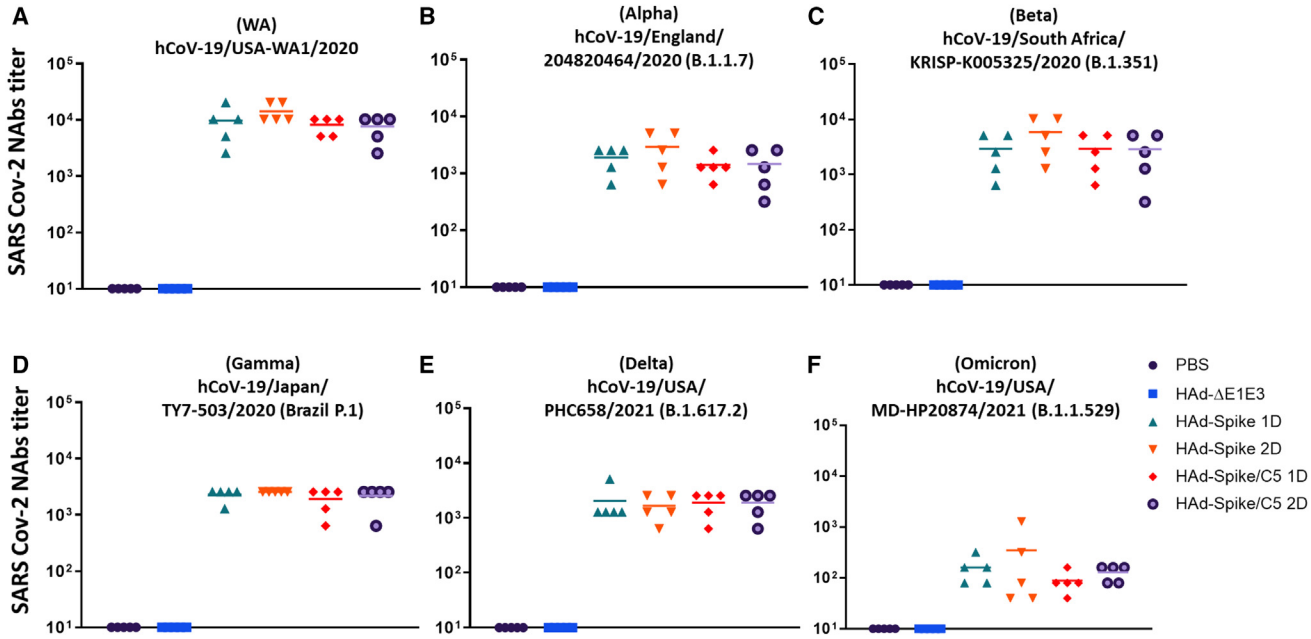

Figure 3. Virus Neutralization (VN) titers against SARS-CoV-2 variants in sera of mice immunized with HAd-Spike or HAd-Spike/C5

Six- to eight-week-old BALB/c mice (5 animals/group were inoculated i.n. with PBS (mock inoculation) or once (1D) or twice (2D) with 10^8 PFUs/animal of HAd-ΔE1E3, HAd-Spike, or HAd-Spike/C5. Four weeks post immunization, blood samples were collected and used to study the development of VN titers against SARS-CoV-2 variants by VN assay. VN assays were performed against original SARS-CoV-2 strain (A), alpha strain (B), Beta strain (C), Gamma strain (D), Delta strain (E), or Omicron strain (F).

lower levels of virus titers in the HAd-Spike/C5-immunized group than in the HAd-Spike-immunized group, but the difference was not statistically significant (Figures 5C–5F).

Protection from lung lesions in golden Syrian hamsters immunized with HAd-Spike or HAd-Spike/C5

To determine the role of vaccination in reducing lesions in the respiratory tract, lung samples from the hamster challenge groups were collected and processed for histopathology 3, 5, 7, and 14 days post infection. Atelectasis, hemorrhage, and congestion were observed throughout the lung sections, even in uninfected controls, and were attributed to euthanasia- or necropsy-associated changes.

In the PBS and HAd-ΔE1E3 groups, there was mild to moderate (day 3) or moderate to marked (day 5) bronchointerstitial pneumonia, characterized by alveolar cell thickening with focal areas of exudation within the septa and alveolar spaces, peribronchiolar inflammation with occasional necrosis of the bronchiolar epithelium, and infiltrates in the lumen of the bronchiole, especially in the PBS group 5 days after infection (Figure 6A). Additionally, moderate to marked vascular changes, characterized by vasculitis, endothelialitis, endothelial hyperplasia, and perivascular edema and inflammation, were seen on day 3 and day 5 after infection (Figure 6B). The extent and severity of interstitial pneumonia and bronchiolitis were significantly reduced in the vaccinated groups. Importantly, no vascular changes were observed in the HAd-Spike/C5 group.

7 days post challenge, in the PBS group, there was severe and diffuse bronchointerstitial pneumonia affecting more than 70% of the lung sections (Figure 6A). Marked peribronchiolitis and exudative and necrotic bronchitis, characterized by peribronchiolar infiltration of inflammatory cells, epithelial cell death, and bronchiolar wall infiltration and desquamation, were observed. Evidence of tissue repair, characterized by type 2 pneumocyte hyperplasia, was also observed. Moderate vascular changes were represented by vasculitis, endothelialitis (mild), endothelial hyperplasia, and perivascular edema and inflammation. There were significant decreases in lung lesions in the vaccinated groups. Tissue repair, characterized by type 2 pneumocyte hyperplasia, was noted in the HAd-Spike/C5-vaccinated group, while minimal hyperplasia was recorded in one animal from the HAd-Spike-vaccinated group.

14 days post challenge, all groups had minimal lung pathology, characterized by occasional peribronchiolar infiltration and focal areas of interstitial inflammation (Figure 6A).

The lung pathology scores for days 3, 5, 7, and 14 showed that vaccinated groups have significantly lower scores than mock- or empty vector-inoculated groups (Figure 7).

DISCUSSION

Ad vectors are considered excellent delivery vehicles for developing vaccines for infectious diseases because of their adjuvant impact through Toll-like receptor (TLR)-dependent and TLR-independent

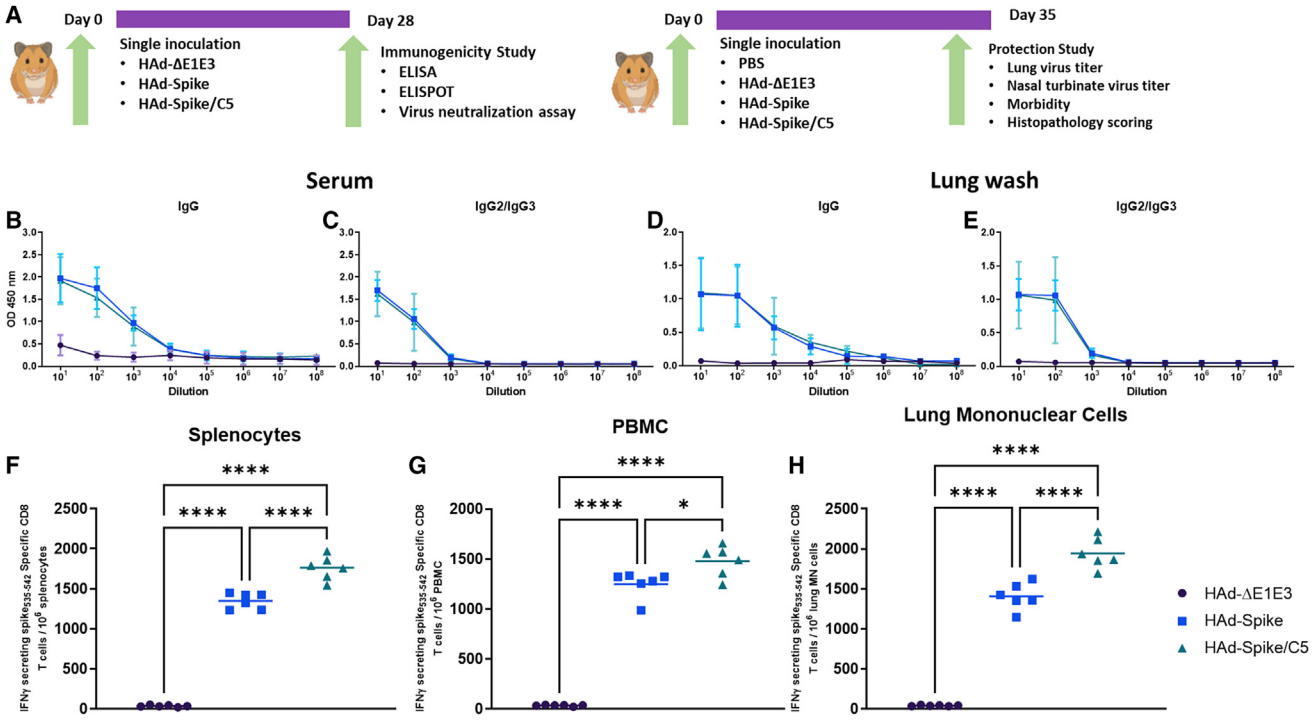

Figure 4. Study design and immunogenicity of HAd-Spike and HAd-Spike/C5 in golden Syrian hamsters

(A) Outlines of the 1D immunogenicity study (right panel) and protection study against SARS-CoV-2 (B.1.1.28) challenge (left panel) following a 1D regimen in the golden Syrian hamster model. Six- to seven-week-old golden Syrian hamsters (3 males and 3 females/group) were inoculated i.n. once with 2×10^8 PFUs/animal of HAd-ΔE1E3, HAd-Spike, or HAd-Spike/C5. (B and C) Four weeks post immunization, blood samples were collected and used to study the development of Spike-specific IgG (B) and IgG2/IgG3 (C) antibody responses by ELISA. (D and E) Similarly, lung washes were used for monitoring the development of Spike-specific IgG (D) and IgG2/IgG3 (E) antibody responses by ELISA. ELISA data are shown as the mean ± SD of the OD readings with log10 diluted samples. (F–H) The development of Spike-specific T cell response after vaccination was investigated in splenocytes (F), peripheral blood MN cells (PBMCs) (G), and lung MN cells (H) by counting Spike-specific IFN-γ-secreting CD8 T cells by ELISpot. *$p \leq 0.05$, ***$p \leq 0.001$, ****$p \leq 0.0001$.

pathways.[31] Four Ad vector-based SARS-CoV-2 vaccines have been used extensively in humans worldwide. These four vaccines are the HAd26-based Johnson & Johnson/Janssen,[32] chimpanzee adenovirus (ChAd)-based AstraZeneca (Vaxzevria),[33] HAd5-based CanSino Biologics, and HAd5- and HAd26-based[34] Gamaleya (prime-boost) vaccines.[35] In addition, the Pfizer-BioNTech[36] and Moderna[37] mRNA-based COVID-19 vaccines and the Bharat Biotech inactivated SARS-CoV-2 vaccine[35] have been widely used globally. Except for the inactivated virus vaccine, all COVID-19 vaccines are based on the S protein, leading to development of virus-neutralizing antibodies. There has been a continuous struggle to handle the emergence of various SARS-CoV-2 variants with increased transmissibility and decreased vaccine efficacy.[38] This study tried to address whether the enhanced Spike-specific T cell response will improve COVID-19 vaccine efficacy. We used AIP-C5 to increase antigen presentation through the autophagy-based pathway. We elucidated previously that AIP-C5 helps with inducing an enhanced T cell response through the autophagy pathway.[24] I.n. inoculation of the HAd-vector or bovine Ad (BAd) vector expressing the Ag85B-p25 epitope and AIP-C5 peptide showed increased levels of effector, central memory, and tissue-resident memory T cells in the lungs of vaccinated mice, indicating development of local immune responses in the lungs. The BAd vector has the advantage of evading HAd pre-existing immunity[39] and is better suited for the i.n. route because of the available sialic acid receptors in the respiratory tract.[40] We used the i.n. route of immunization because this route provided better mucosal protection against the influenza virus, a respiratory infectious agent.[41,42]

Here, we showed that either one or two immunizations of HAd-Spike or HAd-Spike/C5 in mice induced similar levels of humoral (IgG, IgG1, IgG2a, or IgA) immune responses. Nevertheless, the vector containing S with AIP-C5 generated significantly higher levels of T cell immunity, as assessed by enumerating the S-specific IFN-γ-secreting T cells in the spleen and MLN and lung MN cells. We repeated the 1D vaccine study with HAd-Spike or HAd-Spike/C5 in hamsters because they serve as a suitable animal model for SARS-CoV-2 pathogenesis and evaluation of COVID-19 vaccine efficacy. The immunogenicity study in hamsters yielded broadly similar humoral and CMI responses as observed in mice. We have demonstrated previously that antigen-presenting cells infected with an Ad vector expressing a T cell epitope with AIP-C5 resulted in better antigen presentation to CD4 T cells than the Ad vector expressing only

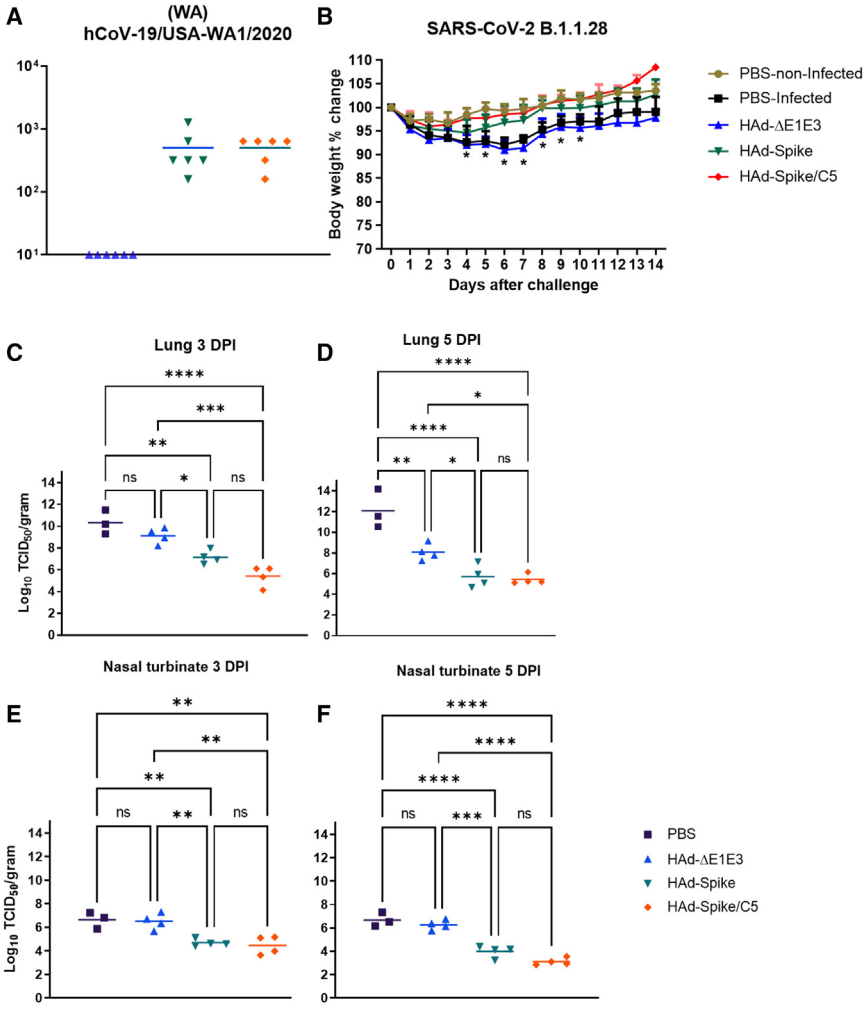

Figure 5. Protection efficacy of a single-dose regimen of HAd-Spike and HAd-Spike/C5 in golden Syrian hamsters

Six- to seven-week-old golden Syrian hamsters were inoculated i.n. once with 2×10^8 PFUs/animal of HAd-ΔE1E3, HAd-Spike, or HAd-Spike/C5. (A) Four weeks post immunization, blood samples were collected and used to study the development of VN titers against SARS-CoV-2 by VN assay. (B) 35 days post immunization, animal groups were challenged with a 10^5 tissue culture infectious dose 50 ($TCID_{50}$) of SARS-CoV-2 (B.1.1.28). Animals were weighed daily for 14 days to monitor morbidity following the challenge. The weight loss or gain percentage with time is shown as a parameter of morbidity. (C–F) Decreases in virus titers in immunized groups following the challenge are shown. Following the challenge, virus titers were determined in the nasal turbinate on days 3 (C) and 5 (D) and in the lungs on days 3 (E) and 5 (F) by $TCID_{50}$ assay. The titers are shown as log 10 $TCID_{50}$/g tissue. ns, $p > 0.05$; *$p \leq 0.05$; **$p \leq 0.01$; ***$p \leq 0.001$; ****$p \leq 0.0001$. DPI, days post infection.

the T cell epitope.[24] The impact seemed to be partly due to autophagy, antigen processing, and lysosomal trafficking. The results of our current study support the hypothesis that AIP-C5 can augment T cell responses other than Mtb antigens in mice and hamsters.

Following vaccination, development of SARS-CoV-2-neutralizing antibody levels and their cross-reactivity against different SARS-CoV-2 variants are considered significant correlates of protection.[26] We observed very high levels ($\sim 10^4$) of virus-neutralizing antibody titers against the homologous strain in mice immunized with HAd-Spike or HAd-Spike/C5 containing the S gene from the Wuhan strain. Cross-neutralizing antibody titers against variant strains (Alpha, Beta, Gamma, and Delta) were reduced by ~1 log but decreased by ~2 logs against an Omicron variant. The inclusion of AIP-C5 did not have a measurable impact on virus-neutralizing antibody titers.

Golden Syrian hamsters, ACE2 transgenic mice, and nonhuman primates are excellent animal models for evaluating SARS-CoV-2 pathogenesis and vaccine efficacy.[28,29] In our study, vaccinated hamsters were challenged with a Gamma variant (B.1.1.28).[43] Our measurable vaccine efficacy considerations included significant decreases in morbidity, virus titers in the respiratory tract, and lung pathology scores. These parameters have been used widely to assess CoV vaccine efficacy in animal models.[44,45] There were significant declines in morbidity, virus titers (in the nasal turbinate and lungs), and lung pathology scores in animal groups immunized with HAd-Spike or HAd-Spike/C5 compared with the control groups. The HAd-Spike/C5 vaccine performed slightly better in reducing morbidity, virus titers, and lung pathology scores than HAd-Spike, but the differences were not statistically significant.

Two HAd5 vector-based COVID-19 vaccines are used in humans as a 2D[9] or HAd5/HAd26-based prime-boost vaccine.[46,47] Because of the high prevalence of HAd5 infection in humans, the pre-existing HAd5 vector immunity may significantly inhibit the development of antigen-specific immune responses.[39,48] Still, the issue of pre-existing vector immunity can be effectively addressed because of the availability of several rare HAd, ChAd, and BAd vectors.[49]

The commercially available ChAdOx1-nCoV-19/AzD1222, containing the S gene with the D614G mutation, was used as an i.n. vaccine in rhesus macaques and hamsters.[50] The i.n. route of vaccination provided significantly higher neutralizing antibody titers than the intramuscular route in hamsters. The neutralizing antibody levels induced in this study were similar to those generated in our current study. Vaccinated hamsters were protected from direct and indirect

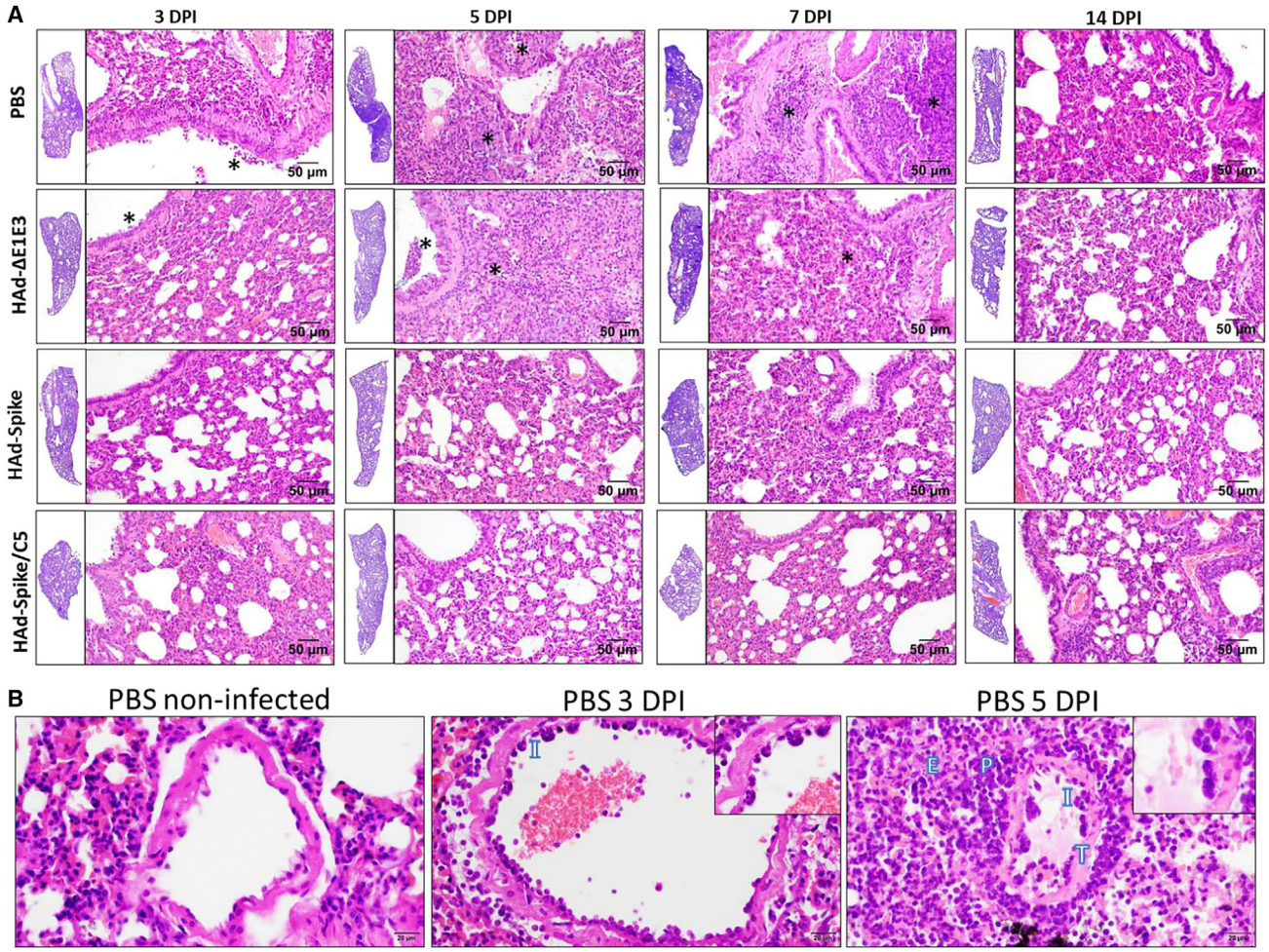

Figure 6. Representative photomicrographs of histopathological lesions of lung tissue sections of golden Syrian hamsters inoculated i.n. with PBS, HAd-ΔE1E3, HAd-Spike, or HAd-Spike/C5 following challenge with SARS-CoV-2

Six- to seven-week-old golden Syrian hamsters were mock inoculated (PBS) or inoculated i.n. once with 2×10^8 PFUs/animal of HAd-ΔE1E3, HAd-Spike, or HAd-Spike/C5. 35 days post immunization, animal groups were challenged with 10^5 $TCID_{50}$ of SARS-CoV-2 (B.1.1.28). (A) Animals were euthanized 3, 5, 7, and 14 days post challenge, and the lung lobe samples were collected and processed for histopathology. The lung tissue sections at low magnification (H&E, 1.5×) are shown as insets on the left side of each higher-magnification photo (H&E, 10×). At low magnification, darker areas correspond to areas with an increased presence of inflammatory cells (exudation). At higher magnification, the asterisks correspond to areas of exudation within the bronchiole and alveolar spaces, which are significantly reduced in the vaccinated groups (HAd-Spike and HAd-Spike/C5) 3, 5, and 7 DPI. 14 DPI, all groups present only minimal exudation. (B) Characteristic histologic features of lung vasculature after challenge with SARS-CoV-2 compared with a PBS-non-infected control (H&E, 20×). Vessels from a PBS-infected animal 3 DPI show moderate vascular changes, vasculitis (I), and endothelialitis (details in inset; H&E, 40×). Vessels from a PBS-infected animal 5 DPI show marked vascular changes, wall thickening (T), vasculitis (I), and endothelialitis (details in inset); note perivascular inflammatory infiltrate (P) and edema (E).

challenges with SARS-CoV-2, as evidenced by significantly lower morbidity and reduced virus load in the nasal swab, bronchoalveolar lavage, and lower respiratory tract compared with the non-vaccinated group.[50]

The correlation of protection against SARS-CoV-2 infection is not yet fully known. The neutralizing antibodies have been shown to correlate with protection and survival from SARS-CoV-2 infection.[51–53] The CMI response against SARS-CoV-2 can protect from severe disease when neutralizing antibody levels are suboptimal.[53,54] Because of significantly higher but similar levels of virus-neutralizing antibody titers with HAd-Spike or HAd-Spike/C5 in hamsters, we could not thoroughly investigate the role of enhanced CMI response in protection.

Developing the next generation of CoV vaccines is critical for better control of the ongoing CoV pandemic. Some requirements of new COVID-19 vaccines include breadth of cross-protection to cover the emerging SARS-CoV-2 variants, durability of vaccine efficacy (at least for 1 year) and a significant reduction in virus

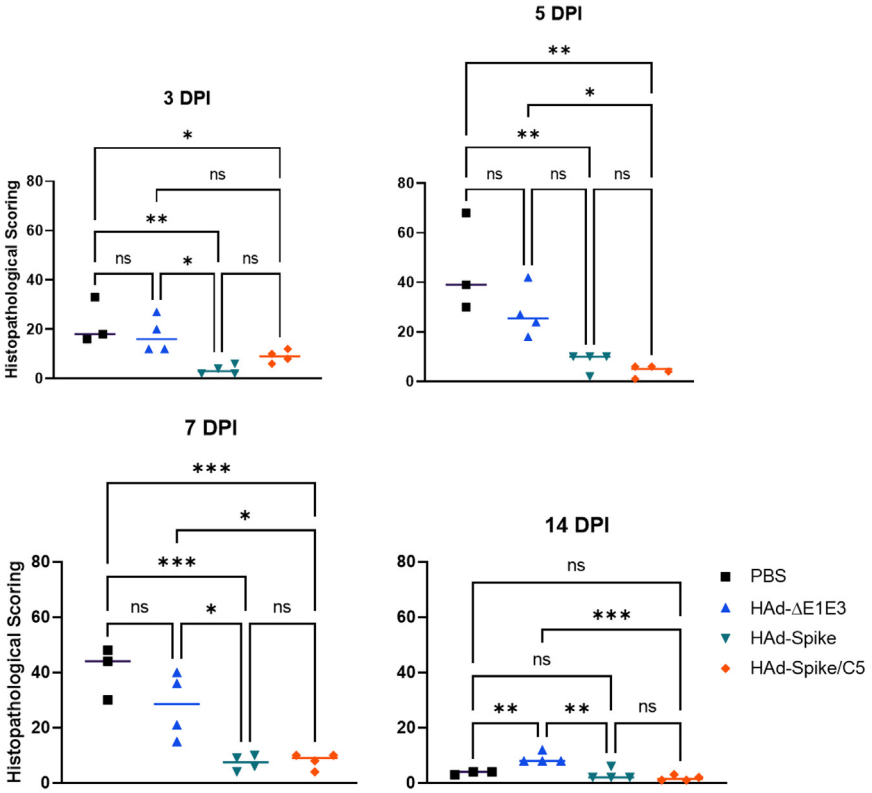

Figure 7. Histopathological scores of the lung tissue sections from HAd-Spike- or HAd-Spike/C5-immunized golden Syrian hamsters following challenge with SARS-CoV-2

Six- to seven-week-old golden Syrian hamsters were mock inoculated (PBS) or inoculated i.n. once with 2×10^8 PFUs/animal of HAd-ΔE1E3, HAd-Spike, or HAd-Spike/C5. 35 days post immunization, animal groups were challenged with 10^5 $TCID_{50}$ of SARS-CoV-2 (B.1.1.28). Animals were euthanized 3, 5, 7, and 14 days post challenge, and the lung lobe samples were collected and processed for histopathology. The tissue sections were scored by a board-certified veterinary pathologist unaware of the animal groups. An in-house-developed scoring system (Table 1) was used to score the lung lesions. ns, $p > 0.05$; *$p \leq 0.05$; **$p \leq 0.01$; ***$p \leq 0.001$.

transmission from vaccinated individuals infected with a variant virus. It has been elucidated that AIP-C5 can induce enhanced memory immune responses;[24] therefore, further studies are required to investigate the durability of protection of HAd-Spike/C5 against various variants, memory B and T cell responses, and the duration and level of virus excretion in vaccinated animals. The role of other SARS-CoV-2 antigens, such as membrane (M) and nucleocapsid (N), in broadening the efficacy of S-based vaccines should be investigated.

MATERIAL AND METHODS

Cell lines

The HEK293 (human embryonic kidney cells expressing HAd5 E1 proteins),[55] 293Cre (293 cells expressing Cre recombinase),[56] BHH2C (bovine-human hybrid clone 2C),[57] and VeroE6 or Vero CCL-81.4 cell lines were grown as monolayer cultures in Corning Dulbecco's modified Eagle's medium (DMEM) (Life Technologies, Thermo Fisher Scientific, Waltham, MA, USA) containing either 10% fetal bovine serum (FBS) or reconstituted FBS (HyClone, Logan, UT, USA) and gentamycin (50 μg/mL).

Ad vectors and SARS-CoV-2 viruses

The S gene of the Wuhan SARS-CoV-2 strain (GenBank: YP_009724390) without or with AIP-C5 was synthesized commercially (GenScript, Piscataway, NJ, USA). The Spike or Spike/C5 gene cassette, under control of the cytomegalovirus (CMV) promoter and bovine growth hormone (BGH) polyadenylation signal, was inserted into the E1 region of the HAd shuttle plasmid. The vectors (HAd-Spike and HAd-Spike/C5) were generated following a Cre-recombinase-mediated site-specific recombination technique as described previously.[58] Generation of HAd-ΔE1E3 (HAd5 with E1 and E3 deletions) has been described previously.[59] Ad vectors were grown in 293 cells and titrated in BBH2C cells, as described earlier.[60] Vectors were purified by cesium chloride density gradient ultracentrifugation following a published protocol.[61]

USA-WA1/2020 (WA) (NR-52281), hCoV-19/England/204820464/2020 (B.1.1.7; Alpha; NR-54000), hCoV-19/South Africa/KRISP-K005325/2020 (lineage B.1.351; Beta; NR-54009), hCoV-19/Brazil/2021 (lineage B.1.1.28.1; Gamma; NR-54982), hCoV-19/USA/PHC658/2021 (lineage B.1.617.2; Delta; NR-55611), and hCoV-19/USA/MD-HP20874/2021 (lineage B.1.1.529; Omicron; NR-56461) were obtained from BEI Resources and grown in Vero E6 cells (CRL-1586, ATCC, USA) and titrated in the same cell line by tissue culture infectious dose 50 ($TCID_{50}$).

Immunogenicity studies in mice and golden Syrian hamsters

All studies were performed in a BSL-2 facility with approval from the Institutional Biosafety Committee (IBC) and the Institutional Animal Care and Use Committee (IACUC) using 6- to 8-week-old BALB/c mice (The Jackson Laboratory, Bar Harbor, ME, USA) and 6- to 7-week-old golden Syrian hamsters (Envigo RMS, Indianapolis, IN, USA).

Mice (5 animals/group, males and females) were mock inoculated (PBS) or inoculated i.n. once or twice (with a 4-week interval) with 10^8 PFUs/animal HAd-ΔE1E3, HAd-Spike, or HAd-Spike/C5. Four weeks post inoculation (1D regimen) or 4 weeks post booster inoculation (2D regimen), animals were anesthetized, blood samples were

Table 1. Semiquantitative histopathological scoring criteria for the lungs of hamsters challenged with SARS-CoV-2

General evaluation	assessment percentage of lung damage area under 4× objective lens	0, none 1, focal lung inflammation within one lobe or <30% of the total lung section 2, diffuse lung inflammation within one lobe or involving 30–70% of the total lung section 3, diffuse lung inflammation involving more than one lobe or 70% of the total lung section
Bronchioles	assessing appearance and severity of peribronchiolar infiltration, intrabronchial wall infiltration, and bronchiolar epithelial cell death/ desquamation	0, none 1, peribronchiolar infiltration 2, bronchiolar epithelial cell death 3, bronchiolar wall infiltration and/or severe epithelium desquamation
Alveoli	assessing the appearance, scope involved, and severity of alveolar septal infiltration, alveolar space infiltration, and alveolar space exudation	0, none 1, only alveolar wall thickening 2, focal area alveolar space infiltration, exudation involving <30% of lung section 3, diffuse alveolar space
Severity of vasculature inflammation	assessing the percentage of vessels affected	0, none 1, only perivascular edema and/or perivascular infiltration 2, mild infiltration within the vessel wall without endothelium infiltration 3, intensive infiltration into the smooth muscle or infiltration beneath the endothelium
Endothelialitis	presence of inflammatory cells beneath or within the endothelial cell layer	0, absent 1, rare 2, common
Endothelial hyperplasia	endothelial cells bulging into the lumen	0, absent 1, rare 2, common
Vasculitis	vessel walls infiltrated with inflammatory cells	0, absent 1, rare 2, common
Mural vascular wall degeneration	hypereosinophilic areas with loss of cell detail	0, absent 1, rare 2, common
Perivascular assessment	perivascular edema or inflammation	0, absent 1, rare 2, common
Repair	tissue repair	0, absent 1, hyperplasia 2, pneumocyte type 2 hyperplasia 3, fibrosis or granulation tissue

Total score = sum of all scores of individual category assessments for each lung section. There were five sections representing different lung lobes. The maximum score possible was 25 × 5 = 125.

obtained via retro-orbital puncture, and lung washes were obtained by homogenizing a lung lobe from each animal in 1 mL of PBS as described previously.[62] The serum samples and lung washes were utilized to assess the development of humoral immune responses. The other lung lobe was processed to collect lung MN cells using lymphocyte separation medium (Corning, Thermo Fisher Scientific) and used to evaluate CMI responses. The spleens and MN nodes were also collected to determine CMI responses.

For the hamster study, animals (6 animals/group, males and females) were inoculated i.n. once with 2×10^8 PFUs/animal of HAd-ΔE1E3, HAd-Spike, or HAd-Spike/C5. Four weeks post inoculation, animals were anesthetized, blood samples were obtained via retro-orbital puncture, and lung washes were obtained by homogenizing one lung from each animal in 1 mL of PBS as described previously.[62] The serum samples and lung washes were utilized to assess the development of humoral immune responses. The second lung was processed to collect lung MN cells using lymphocyte separation medium (Corning, Thermo Fisher Scientific) and used to evaluate CMI responses. The spleens and PBMCs were also collected to assess CMI responses.

Enzyme-linked immunosorbent assay (ELISA)

The assay was performed as described previously.[63,64] Briefly, 96-well ELISA plates (Medisorp and Immulon 2HB, Thermo Fisher

Scientific) were coated with purified RBD of SARS-CoV-2 S protein (NR-52946, BEI Resources; 2 μg/mL). After blocking with 2% bovine serum albumin (BSA) in PBS, diluted serum samples or lung washes (log dilutions) were added and incubated at room temperature for 2 h. After washing with PBS-Tween, the horseradish peroxidase-conjugated goat anti-mouse IgG, IgG1, IgG2a, or IgA antibodies (Invitrogen, Thermo Fisher Scientific) were added at the suggested dilution for each antibody and incubated at room temperature for 2 h, followed by washing four times with PBS-Tween. A BD OptEIA ELISA set (Thermo Fisher Scientific) was used as the substrate. The reaction was stopped with 2 N sulfuric acid solution, and the optical density readings were obtained at 450 nm using a SpectraMax i3x microplate reader (Molecular Devices, Sunnyvale, CA, USA).

ELISpot assay

The IFN-γ ELISpot assay was performed as described earlier.[65] For the mouse study, splenocytes, MLN cells, and lung MN cells were stimulated with a dominant CD8+ cytotoxic T lymphocyte (CTL) epitope (GPKKSTNL)[66] (GenScript). The stimulated cells were processed for the IFN-γ ELISpot assay. For the golden Syrian hamster study, splenocytes, PBMCs, and lung MN cells were used for this assay. The spot-forming units (SFUs) were enumerated using the AID iSpot Advanced Imaging Device (Autoimmun Diagnostika, Strassberg, Germany).

Virus neutralization assay

Virus neutralization (VN) titers of serum samples were quantified by a cell-based assay using the following SARS-CoV-2 strains: USA-WA1/2020 (WA), hCoV-19/England/204820464/2020 (B.1.1.7; Alpha), hCoV-19/South Africa/KRISP-K005325/2020 (lineage B.1.351; Beta), hCoV-19/Brazil/2021 (lineage B.1.1.28.1; Gamma), hCoV-19/USA/PHC658/2021 (lineage B.1.617.2; Delta), and hCoV-19/USA/MD-HP20874/2021 (lineage B.1.1.529; Omicron). Briefly, VeroE6 cells were grown as monolayers in 96-well microtiter plates. Heat-inactivated serum samples were diluted 2-fold in triplicate and incubated with 100 $TCID_{50}$ of the virus in a 5% CO_2 incubator at 37°C for 60 min. This serum-virus mixture was added to cell monolayers and incubated further for 72 h in a 5% CO_2 incubator at 37°C. Plates were visually inspected under a microscope for the presence or absence of cytopathic effect (CPE). The reciprocal of the highest dilution of the sample, where at least two of the three wells showed no CPE, was determined as the VN titer of the sample.

Challenge studies in golden Syrian hamsters

Virus stock and titration

The SARS-CoV-2 strain (SARS-CoV-2/SP02/2020HIAE; GenBank: MT126808.1. B.1.1.28; Gamma) used for the challenge study was initially isolated in VeroE6 cells from a nasopharyngeal sample of one of the first patients infected with SARS-CoV-2 in Brazil.[67] The clinical material was tested by qPCR or qRT-PCR for SARS-CoV-2 and other 15 viral agents (influenza A and B; endemic CoV CoV-NL63, 229E, HKU1, and OC43; enterovirus; parainfluenza virus 1, 2, 3, and 4; metapneumovirus; rhinovirus; respiratory syncytial virus; and Ad).[67] The assays showed positive results only for SARS-CoV-2. The SARS-CoV-2 virus stock was prepared by infecting Vero CCL-81.4 cells with a multiplicity of infection (MOI) of 0.1 for 48 h at 37°C in a 5% CO_2 incubator. The infected cell supernatants were collected and stored at −80°C as virus stock. For titration, virus samples were 10-fold serially diluted (10^{-1}–10^{-12}) in DMEM containing 2.5% FBS and inoculated in sextuplicate in 96-well plates containing 2×10^4 Vero CCL-81.4 cells/well for 72 h at 37°C in a 5% CO_2 incubator for development of viral CPE. For further confirmation, the monolayers were fixed and stained with naphthol blue black (Sigma-Aldrich) solution (0.1% naphthol blue [w/w] with 5.4% acetic acid and 0.7% sodium acetate) and visually inspected under a microscope. Viral titer was calculated using the Spearman and Karber algorithm[68] and expressed as $TCID_{50}$/mL. The isolate used in this study was on its third passage in Vero CCL-81.4 cells.

Animal origin and arrival

Sixty-four conventional male golden Syrian hamsters (*Mesocricetus auratus*, 6–8 weeks old) were acquired from the Instituto Goncalo Muniz (Fiocruz, Salvador, Brazil). Animals were transported in an airplane from Salvador, BA, to São Paulo, SP. Upon arrival, animals were kept in open cages in a negatively pressured room with controlled temperature and humidity at the College of Veterinary Medicine, University of São Paulo, Brazil. Water and food were provided *ad libitum* throughout the experiment. Animals were checked and weighed daily until vaccination.

Grouping and vaccination of the animals

Animals were divided into five groups, homogenized based on body weight. For all i.n. inoculations, hamsters were anesthetized with ketamine (100 mg/kg) and xylazine (5 mg/kg). Group 1 (n = 4) was the mock-inoculated control group and inoculated i.n. with PBS++ (PBS containing 1% $CaCl_2$ and 1% $MgCl_2$) and later mock-infected with DMEM containing 2.5% FBS. Group 2 (n = 12) was inoculated i.n. with PBS++, later infected with 10^5 $TCID_{50}$ of SARS-CoV-2, and served as virus-infected group. Groups 3, 4, and 5 (n = 16 each) were inoculated i.n. once with 2×10^8 PFUs/animal of HAd-ΔE1E3, HAd-Spike, or HAd-Spike/C5, respectively, and later challenged with 10^5 $TCID_{50}$ of SARS-CoV-2.

Animal transfer to an animal biosafety level 3 laboratory (ABSL3)

Animals were transferred to ABSL3 of the Institute of Biomedical Sciences, University of São Paulo, Brazil. They were kept in pairs in ABSL3 microisolators and provided water and food *ad libitum*. The acclimatization period was 7 days. Animals were observed for clinical signs and weighed daily, with disinfection of the biosafety cabinet between the groups.

SARS-CoV-2 challenge and follow-up

Animals received 2 mg/kg of morphine subcutaneously (s.c.), and after 20 min were anesthetized with ketamine (100 mg/kg) and xylazine (5 mg/kg) intraperitoneally (i.p.). Blood samples were collected from all animals before inoculation, and then groups 2, 3, 4, and 5 received 10^5 $TCID_{50}$/animal of SARS-CoV-2 (B.1.1.28) i.n. Animals were monitored for clinical signs and weighed daily. Weight loss or gain

for each animal was calculated as the percentage weight loss or gain compared with the weight on day 0 and expressed as the mean ± standard deviation.

Euthanasia, necropsy, and sample collection

Three or four animals per group were euthanized 3, 5, 7, and 14 days post infection with an overdose of ketamine (600 mg/kg) and xylazine (30 mg/kg, i.p.) after morphine inoculation (5 mg/kg, s.c.). Blood samples were collected through heart puncture. Sterile instruments were changed between organ collection (nasal turbinate and lungs) to avoid cross-contamination. The biosafety cabinet was disinfected with 70% ethanol after handling animals from each group. Lung lobes (5 samples) were collected separately for histopathology in 10% formalin. The nasal turbinate and lung samples were collected for virus load quantification in DMEM containing penicillin, streptomycin, and 1-mm glass beads. Organ samples were individually weighed, rapidly frozen in liquid nitrogen, and then transferred to −80°C.

Virus load quantification

Virus load quantification was performed by determining $TCID_{50}$/mL/g of tissue. The nasal turbinate and lung samples were thawed and subjected to disruption with 1-mm glass beads using a QIAGEN Tissue Lyser II at 50 Hz twice for 2 min, followed by centrifugation at 2,000 × *g* for 30 s. Supernatants were used for virus titration as described above, and the results were expressed as $TCID_{50}$/mL/g of tissue.

Histopathological analysis

Formalin-fixed lung samples were subjected to routine fixation, paraffin embedding, sectioning, and staining with hematoxylin and eosin (H&E). A board-certified pathologist (Dr. Andrea Santos, Purdue University), who was not associated with the study design, examined the stained lung tissue sections under a light microscope for the presence of the SARS-CoV-2-induced lesions that have been described in the literature[69–71] and scored according to an in-house-developed scoring system (Table 1). All five lung lobes were analyzed separately (right cranial lobe, right middle lobe, right caudal lobe, accessory lobe, and left lung).

Statistical analyses

The statistical significance was set at $p < 0.05$. One-way ANOVA with Bonferroni post-test was used to ascertain statistical significance.

DATA AVAILABILITY

All data will be available upon request to the corresponding author.

ACKNOWLEDGMENTS

All animal experiments were conducted following the approval and guidelines of the Institutional Animal Care and Use Committee (IACUC), the Institutional Biosafety Committee (IBC), and the Institute of Biomedical Sciences and College of Veterinary Medicine, University of São Paulo, protocols 5167261020 and 7271131020. This work was supported by Public Health Service grant AI059374 from the National Institute of Allergy and Infectious Diseases and the USDA National Institute of Food and Agriculture (Hatch 1014146). This work was also supported by the São Paulo Research Foundation (FAPESP, 2020/07251-2). M.V.A.'s fellowship was funded by the Butantan Foundation, São Paulo, Brazil. T.T.S.-P.'s fellowship was funded by CAPES, Ministry of Education, Brazil (88887.508739/2020, 001). The fellowships of A.F.d.S.F., M.S.T., M.C.A., C.L.S., and D.M.d.F. were funded by FAPESP (2020/09149-0, 2021/02736-0, 2019/12691-4, 2019/13916-0, and 2015/364-0, 2021/06881-5, respectively). The following reagent was produced under HHSN272201400008C and obtained through BEI Resources, NIAID, NIH: Spike glycoprotein receptor binding domain (RBD) from SARS-related coronavirus 2, USA-WA1/2020 virus, hCoV-19/England/204820464/2020 (B.1.1.7), hCoV-19/South Africa/KRISP-K005325/2020 (lineage B.1.351), hCoV-19/Japan/TY7-503/2021 (Brazil P.1), hCoV-19/USA/PHC658/2021 (lineage B.1.617.2), and hCoV-19/USA/MD-HP20874/2021 (lineage B.1.1.529).

AUTHOR CONTRIBUTIONS

E.E.S., M.V.A., T.T.S.-P., S.K.C., A.E., M.A., W.-C.W., M.S.N., A.G., R.N., A.F.d.S.F., M.S.T., M.C.A., C.L.S., D.M.d.F., E.D.d.O.C., D.B.L.O., E.L.D., M.B.H., D.M.d.F., and A.M.S.G. performed the experiments. S.V.K., A.M.S.G., and S.K.M. designed the study. C.J. provided AIP-C5-related expertise. A.P.S. performed histopathologic evaluations.

DECLARATION OF INTERESTS

The authors declare no competing interests.

REFERENCES

1. Wang, C., Horby, P.W., Hayden, F.G., and Gao, G.F. (2020). A novel coronavirus outbreak of global health concern. Lancet *395*, 470–473. https://doi.org/10.1016/s0140-6736(20)30185-9.
2. COVID Live (2022). Coronavirus Statistics - Worldometer. https://www.worldometers.info/coronavirus/.
3. Ahmed, S., Khan, S., Imran, I., Al Mughairbi, F., Sheikh, F.S., Hussain, J., Khan, A., and Al-Harrasi, A. (2021). Vaccine development against COVID-19: study from pre-clinical phases to clinical trials and global use. Vaccines *9*, e080836. https://doi.org/10.3390/vaccines9080836.
4. (2022). COVID-19 Vaccine Tracker and Landscape. https://www.who.int/publications/m/item/draft-landscape-of-covid-19-candidate-vaccines.
5. Niazi, S.K. (2022). Making COVID-19 mRNA vaccines accessible: challenges resolved. Expert Rev. Vaccines *21*, 1163–1176. https://doi.org/10.1080/14760584.2022.2089121.
6. Sheridan, C. (2021). First COVID-19 DNA vaccine approved, others in hot pursuit. Nat. Biotechnol. 1479–1482. https://doi.org/10.1038/d41587-021-00023-5.
7. (2022). COVAXIN® (BBV152) – Inactivated, COVID-19 Vaccine. https://www.who.int/publications/m/item/covaxin-(bbv152)-inactivated-covid-19-vaccine.
8. (2022). CDC Recommends Novavax's COVID-19 Vaccine for Adults | CDC Online Newsroom | CDC. https://www.cdc.gov/media/releases/2022/s0719-covid-novavax-vaccine.html.
9. Mendonça, S.A., Lorincz, R., Boucher, P., and Curiel, D.T. (2021). Adenoviral vector vaccine platforms in the SARS-CoV-2 pandemic. NPJ Vaccines *6*, 97. https://doi.org/10.1038/s41541-021-00356-x.
10. Zhou, H., Chen, X., Hu, T., Li, J., Song, H., Liu, Y., Wang, P., Liu, D., Yang, J., Holmes, E.C., et al. (2020). A Novel Bat Coronavirus Closely Related to SARS-CoV-2 Contains Natural Insertions at the S1/S2 Cleavage Site of the Spike Protein. Curr. Biol. *30*, 2196–2203.e3. https://doi.org/10.1016/j.cub.2020.05.023.
11. Hoffmann, M., Kleine-Weber, H., Schroeder, S., Krüger, N., Herrler, T., Erichsen, S., Schiergens, T.S., Herrler, G., Wu, N.H., Nitsche, A., et al. (2020). SARS-CoV-2 cell entry depends on ACE2 and TMPRSS2 and is blocked by a Clinically Proven Protease Inhibitor. Cell *181*, 271–280.e8. https://doi.org/10.1016/j.cell.2020.02.052.

12. Ou, X., Liu, Y., Lei, X., Li, P., Mi, D., Ren, L., Guo, L., Guo, R., Chen, T., Hu, J., et al. (2020). Characterization of spike glycoprotein of SARS-CoV-2 on virus entry and its immune cross-reactivity with SARS-CoV. Nat. Commun. *11*, 1620. https://doi.org/10.1038/s41467-020-15562-9.

13. Lan, J., Ge, J., Yu, J., Shan, S., Zhou, H., Fan, S., Zhang, Q., Shi, X., Wang, Q., Zhang, L., and Wang, X. (2020). Structure of the SARS-CoV-2 spike receptor-binding domain bound to the ACE2 receptor. Nature *581*, 215–220. https://doi.org/10.1038/s41586-020-2180-5.

14. Shang, J., Ye, G., Shi, K., Wan, Y., Luo, C., Aihara, H., Geng, Q., Auerbach, A., and Li, F. (2020). Structural basis of receptor recognition by SARS-CoV-2. Nature *581*, 221–224. https://doi.org/10.1038/s41586-020-2179-y.

15. Yuan, M., Wu, N.C., Zhu, X., Lee, C.C.D., So, R.T.Y., Lv, H., Mok, C.K.P., and Wilson, I.A. (2020). A highly conserved cryptic epitope in the receptor binding domains of SARS-CoV-2 and SARS-CoV. Science *368*, 630–633. https://doi.org/10.1126/science.abb7269.

16. Letko, M., Marzi, A., and Munster, V. (2020). Functional assessment of cell entry and receptor usage for SARS-CoV-2 and other lineage B betacoronaviruses. Nat. Microbiol. *5*, 562–569. https://doi.org/10.1038/s41564-020-0688-y.

17. Li, Y., Zhang, Z., Yang, L., Lian, X., Xie, Y., Li, S., Xin, S., Cao, P., and Lu, J. (2020). The MERS-CoV receptor DPP4 as a candidate binding target of the SARS-CoV-2 spike. iScience *23*, 101160. https://doi.org/10.1016/j.isci.2020.101160.

18. Grifoni, A., Weiskopf, D., Ramirez, S.I., Mateus, J., Dan, J.M., Moderbacher, C.R., Rawlings, S.A., Sutherland, A., Premkumar, L., Jadi, R.S., et al. (2020). Targets of T cell responses to SARS-CoV-2 coronavirus in humans with COVID-19 disease and unexposed individuals. Cell *181*, 1489–1501.e15. https://doi.org/10.1016/j.cell.2020.05.015.

19. Harvey, W.T., Carabelli, A.M., Jackson, B., Gupta, R.K., Thomson, E.C., Harrison, E.M., Ludden, C., Reeve, R., Rambaut, A., COVID-19 Genomics UK COG-UK Consortium, Peacock, S.J., and Robertson, D.L. (2021). SARS-CoV-2 variants, spike mutations and immune escape. Nat. Rev. Microbiol. *19*, 409–424. https://doi.org/10.1038/s41579-021-00573-0.

20. (2022). SARS-CoV-2 Variant Classifications and Definitions. https://www.cdc.gov/coronavirus/2019-ncov/variants/variant-classifications.html.

21. Takashita, E., Kinoshita, N., Yamayoshi, S., Sakai-Tagawa, Y., Fujisaki, S., Ito, M., Iwatsuki-Horimoto, K., Chiba, S., Halfmann, P., Nagai, H., et al. (2022). Efficacy of antibodies and antiviral drugs against Covid-19 Omicron variant. N. Engl. J. Med. *386*, 995–998. https://doi.org/10.1056/NEJMc2119407.

22. Araf, Y., Akter, F., Tang, Y.D., Fatemi, R., Parvez, M.S.A., Zheng, C., and Hossain, M.G. (2022). Omicron variant of SARS-CoV-2: genomics, transmissibility, and responses to current COVID-19 vaccines. J. Med. Virol. *94*, 1825–1832. https://doi.org/10.1002/jmv.27588.

23. Zhou, W., and Wang, W. (2021). Fast-spreading SARS-CoV-2 variants: challenges to and new design strategies of COVID-19 vaccines. Signal Transduct. Target. Ther. *6*, 226. https://doi.org/10.1038/s41392-021-00644-x.

24. Khan, A., Sayedahmed, E.E., Singh, V.K., Mishra, A., Dorta-Estremera, S., Nookala, S., Canaday, D.H., Chen, M., Wang, J., Sastry, K.J., et al. (2021). A recombinant bovine adenoviral mucosal vaccine expressing mycobacterial antigen-85B generates robust protection against tuberculosis in mice. Cell Rep. Med. *2*, 100372. https://doi.org/10.1016/j.xcrm.2021.100372.

25. Sayedahmed, E.E., Andrea, P., dos Santos1, Jagannath, C., Sambhara, S., and Mittal, S.K. (2022). An autophagy-inducing peptide enhances cell-mediated immune responses of an adenoviral vector-based vaccine expressing H7N9 nucleoprotein and confers protection against H1N1, H3N2, H5N2, H7N9 and H9N2 influenza A viruses. Under Reviewing.

26. Khoury, D.S., Cromer, D., Reynaldi, A., Schlub, T.E., Wheatley, A.K., Juno, J.A., Subbarao, K., Kent, S.J., Triccas, J.A., and Davenport, M.P. (2021). Neutralizing antibody levels are highly predictive of immune protection from symptomatic SARS-CoV-2 infection. Nat. Med. *27*, 1205–1211. https://doi.org/10.1038/s41591-021-01377-8.

27. Cromer, D., Steain, M., Reynaldi, A., Schlub, T.E., Wheatley, A.K., Juno, J.A., Kent, S.J., Triccas, J.A., Khoury, D.S., and Davenport, M.P. (2022). Neutralising antibody titres as predictors of protection against SARS-CoV-2 variants and the impact of boosting: a meta-analysis. Lancet. Microbe *3*, e52–e61. https://doi.org/10.1016/s2666-5247(21)00267-6.

28. Rosenke, K., Meade-White, K., Letko, M., Clancy, C., Hansen, F., Liu, Y., Okumura, A., Tang-Huau, T.L., Li, R., Saturday, G., et al. (2020). Defining the Syrian hamster as a highly susceptible preclinical model for SARS-CoV-2 infection. Emerg. Microbes Infect. *9*, 2673–2684. https://doi.org/10.1080/22221751.2020.1858177.

29. Le Bras, A. (2020). Syrian hamsters as a small animal model for COVID-19 research. Lab Anim. *49*, 223. https://doi.org/10.1038/s41684-020-0614-1.

30. Coe, J.E., Schell, R.F., and Ross, M.J. (1995). Immune response in the hamster: definition of a novel IgG not expressed in all hamster strains. Immunology *86*, 141–148.

31. Zhu, J., Huang, X., and Yang, Y. (2007). Innate immune response to adenoviral vectors is mediated by both Toll-like receptor-dependent and -independent pathways. J. Virol. *81*, 3170–3180. https://doi.org/10.1128/jvi.02192-06.

32. @US_FDA (2022). Janssen COVID-19 Vaccine | FDA. https://www.fda.gov/emergency-preparedness-and-response/coronavirus-disease-2019-covid-19/janssen-covid-19-vaccine.

33. (2022). Vaxzevria (Previously COVID-19 Vaccine AstraZeneca) (European Medicines Agency). https://www.ema.europa.eu/en/medicines/human/EPAR/vaxzevria-previously-covid-19-vaccine-astrazeneca.

34. Burki, T.K. (2020). The Russian vaccine for COVID-19. The Lancet. Lancet Respir. Med. *8*, e85–e86. https://doi.org/10.1016/s2213-2600(20)30402-1.

35. CDC (2020). COVID Data Tracker. https://covid.cdc.gov/covid-data-tracker.

36. @US_FDA (2021). FDA Approves First COVID-19 Vaccine | FDA. https://www.fda.gov/news-events/press-announcements/fda-approves-first-covid-19-vaccine.

37. @US_FDA (2022). Coronavirus (COVID-19) Update: FDA Takes Key Action by Approving Second COVID-19 Vaccine | FDA. https://www.fda.gov/news-events/press-announcements/coronavirus-covid-19-update-fda-takes-key-action-approving-second-covid-19-vaccine.

38. Krause, P.R., Fleming, T.R., Longini, I.M., Peto, R., Briand, S., Heymann, D.L., Beral, V., Snape, M.D., Rees, H., Ropero, A.M., et al. (2021). SARS-CoV-2 Variants and Vaccines. N. Engl. J. Med. *385*, 179–186. https://doi.org/10.1056/NEJMsr2105280.

39. Singh, N., Pandey, A., Jayashankar, L., and Mittal, S.K. (2008). Bovine adenoviral vector-based H5N1 influenza vaccine overcomes exceptionally high levels of pre-existing immunity against human adenovirus. Mol. Ther. *16*, 965–971. https://doi.org/10.1038/mt.2008.12.

40. Li, X., Bangari, D.S., Sharma, A., and Mittal, S.K. (2009). Bovine adenovirus serotype 3 utilizes sialic acid as a cellular receptor for virus entry. Virology *392*, 162–168. https://doi.org/10.1016/j.virol.2009.06.029.

41. Vemula, S.V., and Mittal, S.K. (2010). Production of adenovirus vectors and their use as a delivery system for influenza vaccines. Expert Opin. Biol. Ther. *10*, 1469–1487. https://doi.org/10.1517/14712598.2010.519332.

42. Sayedahmed, E.E., Hassan, A.O., Kumari, R., Cao, W., Gangappa, S., York, I., Sambhara, S., and Mittal, S.K. (2018). A bovine adenoviral vector-based H5N1 influenza -vaccine provides enhanced immunogenicity and protection at a significantly low dose. Mol. Ther. Methods Clin. Dev. *10*, 210–222. https://doi.org/10.1016/j.omtm.2018.07.007.

43. (2022). CoVariants. https://covariants.org/.

44. Wang, S., Li, L., Yan, F., Gao, Y., Yang, S., and Xia, X. (2021). COVID-19 animal models and vaccines: current landscape and future prospects. Vaccines *9*, e101082. https://doi.org/10.3390/vaccines9101082.

45. Muñoz-Fontela, C., Dowling, W.E., Funnell, S.G.P., Gsell, P.S., Riveros-Balta, A.X., Albrecht, R.A., Andersen, H., Baric, R.S., Carroll, M.W., Cavaleri, M., et al. (2020). Animal models for COVID-19. Nature *586*, 509–515. https://doi.org/10.1038/s41586-020-2787-6.

46. (2022). COVID-19 Vaccine Tracker. https://www.raps.org/news-and-articles/news-articles/2020/3/covid-19-vaccine-tracker.

47. Logunov, D.Y., Dolzhikova, I.V., Shcheblyakov, D.V., Tukhvatulin, A.I., Zubkova, O.V., Dzharullaeva, A.S., Kovyrshina, A.V., Lubenets, N.L., Grousova, D.M., Erokhova, A.S., et al.; Gam-COVID-Vac Vaccine Trial Group (2021). Safety and efficacy of an rAd26 and rAd5 vector-based heterologous prime-boost COVID-19

vaccine: an interim analysis of a randomised controlled phase 3 trial in Russia. Lancet *397*, 671–681. https://doi.org/10.1016/s0140-6736(21)00234-8.

48. Fausther-Bovendo, H., and Kobinger, G.P. (2014). Pre-existing immunity against Ad vectors: humoral, cellular, and innate response, what's important? Hum. Vaccin. Immunother. *10*, 2875–2884. https://doi.org/10.4161/hv.29594.

49. Mittal, S.K., Ahi, Y.S., and Vemula, S.V. (2016). 19 - Xenogenic Adenoviral Vectors A2 - Curiel, David T. In Adenoviral Vectors for Gene Therapy, 2nd ed. (San Diego: Academic Press), pp. 495–528. https://doi.org/10.1016/B978-0-12-800276-6.00019-X.

50. van Doremalen, N., Purushotham, J.N., Schulz, J.E., Holbrook, M.G., Bushmaker, T., Carmody, A., Port, J.R., Yinda, C.K., Okumura, A., Saturday, G., et al. (2021). Intranasal ChAdOx1 nCoV-19/AZD1222 vaccination reduces viral shedding after SARS-CoV-2 D614G challenge in preclinical models. Sci. Transl. Med. *13*, eabh0755. https://doi.org/10.1126/scitranslmed.abh0755.

51. Garcia-Beltran, W.F., Lam, E.C., Astudillo, M.G., Yang, D., Miller, T.E., Feldman, J., Hauser, B.M., Caradonna, T.M., Clayton, K.L., Nitido, A.D., et al. (2021). COVID-19-neutralizing antibodies predict disease severity and survival. Cell *184*, 476–488.e11. https://doi.org/10.1016/j.cell.2020.12.015.

52. Addetia, A., Crawford, K.H.D., Dingens, A., Zhu, H., Roychoudhury, P., Huang, M.L., Jerome, K.R., Bloom, J.D., and Greninger, A.L. (2020). Neutralizing Antibodies Correlate with Protection from SARS-CoV-2 in Humans during a Fishery Vessel Outbreak with a High Attack Rate. J. Clin. Microbiol. *58*, e02107-20. https://doi.org/10.1128/jcm.02107-20.

53. McMahan, K., Yu, J., Mercado, N.B., Loos, C., Tostanoski, L.H., Chandrashekar, A., Liu, J., Peter, L., Atyeo, C., Zhu, A., et al. (2021). Correlates of protection against SARS-CoV-2 in rhesus macaques. Nature *590*, 630–634. https://doi.org/10.1038/s41586-020-03041-6.

54. Goldblatt, D., Alter, G., Crotty, S., and Plotkin, S.A. (2022). Correlates of protection against SARS-CoV-2 infection and COVID-19 disease. Immunol. Rev. *310*, 6–26. https://doi.org/10.1111/imr.13091.

55. Graham, F.L., Smiley, J., Russell, W.C., and Nairn, R. (1977). Characteristics of a human cell line transformed by DNA from human adenovirus type 5. J. Gen. Virol. *36*, 59–74. https://doi.org/10.1099/0022-1317-36-1-59.

56. Chen, L., Anton, M., and Graham, F.L. (1996). Production and characterization of human 293 cell lines expressing the site-specific recombinase Cre. Somat. Cell Mol. Genet. *22*, 477–488.

57. van Olphen, A.L., and Mittal, S.K. (2002). Development and characterization of bovine x human hybrid cell lines that efficiently support the replication of both wild-type bovine and human adenoviruses and those with E1 deleted. J. Virol. *76*, 5882–5892.

58. Sayedahmed, E.E., Kumari, R., and Mittal, S.K. (2019). Current use of adenovirus vectors and their production methods. In Viral Vectors for Gene Therapy: Methods and Protocols, F.P. Manfredsson and M.J. Benskey, eds. (Springer New York), pp. 155–175. https://doi.org/10.1007/978-1-4939-9065-8_9.

59. Noblitt, L.W., Bangari, D.S., Shukla, S., Knapp, D.W., Mohammed, S., Kinch, M.S., and Mittal, S.K. (2004). Decreased tumorigenic potential of EphA2-overexpressing breast cancer cells following treatment with adenoviral vectors that express EphrinA1. Cancer Gene Ther. *11*, 757–766. https://doi.org/10.1038/sj.cgt.7700761.

60. Vemula, S.V., Ahi, Y.S., Swaim, A.M., Katz, J.M., Donis, R., Sambhara, S., and Mittal, S.K. (2013). Broadly protective adenovirus-based multivalent vaccines against highly pathogenic avian influenza viruses for pandemic preparedness. PLoS One *8*, e62496. https://doi.org/10.1371/journal.pone.0062496.

61. Pandey, A., Singh, N., Vemula, S.V., Couëtil, L., Katz, J.M., Donis, R., Sambhara, S., and Mittal, S.K. (2012). Impact of preexisting adenovirus vector immunity on immunogenicity and protection conferred with an adenovirus-based H5N1 influenza vaccine. PLoS One *7*, e33428. https://doi.org/10.1371/journal.pone.0033428.

62. Papp, Z., Middleton, D.M., Mittal, S.K., Babiuk, L.A., and Baca-Estrada, M.E. (1997). Mucosal immunization with recombinant adenoviruses: induction of immunity and protection of cotton rats against respiratory bovine herpesvirus type 1 infection. J. Gen. Virol. *78*, 2933–2943. https://doi.org/10.1099/0022-1317-78-11-2933.

63. Mittal, S.K., Middleton, D.M., Tikoo, S.K., and Babiuk, L.A. (1995). Pathogenesis and immunogenicity of bovine adenovirus type 3 in cotton rats (Sigmodon hispidus). Virology *213*, 131–139. https://doi.org/10.1006/viro.1995.1553.

64. Mittal, S.K., Aggarwal, N., Sailaja, G., van Olphen, A., HogenEsch, H., North, A., Hays, J., and Moffatt, S. (2000). Immunization with DNA, adenovirus or both in biodegradable alginate microspheres: effect of route of inoculation on immune response. Vaccine *19*, 253–263.

65. Hoelscher, M.A., Garg, S., Bangari, D.S., Belser, J.A., Lu, X., Stephenson, I., Bright, R.A., Katz, J.M., Mittal, S.K., and Sambhara, S. (2006). Development of adenoviral-vector-based pandemic influenza vaccine against antigenically distinct human H5N1 strains in mice. Lancet *367*, 475–481. https://doi.org/10.1016/S0140-6736(06)68076-8.

66. Muraoka, D., Situo, D., Sawada, S.I., Akiyoshi, K., Harada, N., and Ikeda, H. (2020). Identification of a dominant CD8(+) CTL epitope in the SARS-associated coronavirus 2 spike protein. Vaccine *38*, 7697–7701. https://doi.org/10.1016/j.vaccine.2020.10.039.

67. Araujo, D.B., Machado, R.R.G., Amgarten, D.E., Malta, F.d.M., de Araujo, G.G., Monteiro, C.O., Candido, E.D., Soares, C.P., de Menezes, F.G., Pires, A.C.C., et al. (2020). SARS-CoV-2 isolation from the first reported patients in Brazil and establishment of a coordinated task network. Mem. Inst. Oswaldo Cruz *115*, e200342. https://doi.org/10.1590/0074-02760200342.

68. Hierholzer, J.C., and Killington, R.A. (1996). 2 - Virus isolation and quantitation. In Virol Methods Man, B.W.J. Mahy and H.O. Kangro, eds. (Academic Press), pp. 25–46. https://doi.org/10.1016/B978-012465330-6/50003-8.

69. Imai, M., Iwatsuki-Horimoto, K., Hatta, M., Loeber, S., Halfmann, P.J., Nakajima, N., Watanabe, T., Ujie, M., Takahashi, K., Ito, M., et al. (2020). Syrian hamsters as a small animal model for SARS-CoV-2 infection and countermeasure development. Proc. Natl. Acad. Sci. USA *117*, 16587–16595. https://doi.org/10.1073/pnas.2009799117.

70. Chan, J.F.W., Zhang, A.J., Yuan, S., Poon, V.K.M., Chan, C.C.S., Lee, A.C.Y., Chan, W.M., Fan, Z., Tsoi, H.W., Wen, L., et al. (2020). Simulation of the clinical and pathological manifestations of Coronavirus Disease 2019 (COVID-19) in a Golden Syrian Hamster Model: implications for disease pathogenesis and transmissibility. Clin. Infect. Dis. *71*, 2428–2446. https://doi.org/10.1093/cid/ciaa325.

71. Pandey, K., Acharya, A., Mohan, M., Ng, C.L., Reid, S.P., and Byrareddy, S.N. (2021). Animal models for SARS-CoV-2 research: a comprehensive literature review. Transbound. Emerg. Dis. *68*, 1868–1885. https://doi.org/10.1111/tbed.13907.